

## Structural and magnetic properties of Fe–Ni mecanosynthesized alloys

J. F. Valderruten · G. A. Pérez Alcázar ·  
J. M. Greneche

Published online: 25 September 2009  
© Springer Science + Business Media B.V. 2009

**Abstract** Fe<sub>100-x</sub>Ni<sub>x</sub> samples with  $x = 22.5, 30.0$  and  $40.0$  at.% Ni were prepared by mechanical alloying (MA) with milling times of 10, 24, 48 and 72 h, a ball mass to powder mass (BM/PM) ratio of 20:1 and rotation velocity of 280 rev/min. Then the samples were sintered at 1,000°C and characterized by X-ray diffraction (XRD) and transmission Mössbauer spectrometry (TMS). From the refinement of the X ray patterns we found in this composition range two crystalline phases, one body centered cubic (BCC), one face centered cubic (FCC) and some samples show FeO and Fe<sub>3</sub>O<sub>4</sub> phases. The obtained grain size of the samples shows their nanostructured character. Mössbauer spectra were fitted using a model with two hyperfine magnetic field distributions (HMFDs), and a narrow singlet. One hyperfine field distribution corresponds to the ferromagnetic BCC grains, the other to the ferromagnetic FCC grains (Taenite), and the narrow singlet to the paramagnetic FCC grains (antitaenite). Some samples shows a paramagnetic doublet which corresponds to FeO and two sextets corresponding to the ferrimagnetic Fe<sub>3</sub>O<sub>4</sub> phase. In this fit model we used a texture correction in order to take into account the interaction between the particles with flake shape and the Mössbauer  $\gamma$ -rays.

**Keywords** Invar alloys · Magnetic nanostructured powders · Mechanical alloying · Mössbauer spectrometry · X-ray diffraction

**PACS** 64.70.ND · 76.80.\_Y · 75.50.TT · 61.05.CP

---

J. F. Valderruten (✉) · G. A. Pérez Alcázar  
Departamento de Física, Universidad del Valle, A. A. 25360, Cali, Colombia  
e-mail: jfvalder@yahoo.com

J. M. Greneche  
Laboratoire de Physique de l'Etat Condensé, UMR CNRS 6087, Université du Maine,  
72085 Le Mans, Cedex 9, France

## 1 Introduction

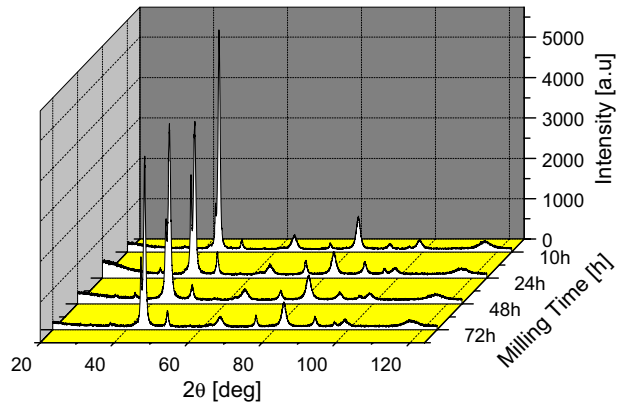
Fe–Ni system has attracted the attention of researchers because it originates the formation of a great number of alloys with special thermal and magnetic properties [1–14]. The use of high energy mills and other new technological methods of preparation joined, in some cases, by heat treatments, enable to obtain samples with different structures and novel properties. This is the current field of the nanotechnology, which allows preparing nanostructured Fe–Ni alloys and other different materials [15, 16]. Their small grain size gives rise to a high ratio between the number of atoms located in the grain boundary and those in the interior. In addition, these materials are very interesting from the magnetic point of view because their reduced grain size approaches to the size of a magnetic domain and offer the possibility to eliminate the influence of the domain walls. It is very well established that the intermetallic compounds prepared by mechanical alloying (MA) have a high structural disorder and are unstable [17–19]. These factors implied unusual physical properties, which are very different compared with those of bulk microcrystalline materials. For this reason, several studies have been carried out investigating the structural properties of the Fe–Ni alloys prepared by MA [6, 7]. Kaloshkin et al. [12], after annealing at 650°C samples of the  $\text{Fe}_{1-x}\text{Ni}_x$  system prepared by MA, showed that the concentration ranges of the phase existence shift to the low nickel content side of the phase diagram of melted alloys, and additionally showed the formation of a non-ferromagnetic alloys very unusual for the Fe–Ni system. More recently Valderruten et al. [20] have reported a MS and XRD study of samples from the  $\text{Fe}_{100-x}\text{Ni}_x$  system, with  $x$  varying from 22.5 up to 40, prepared by MA. They found that all the samples present the coexistence of some phases: the ferromagnetic Fe–Ni BCC, the ferromagnetic Fe–Ni FCC (taenite) and the paramagnetic Fe–Ni FCC phase (antitaenite). They proposed a new fit model which includes two HMFDS which correspond to the two ferromagnetic phases and a paramagnetic site which corresponds to the antitaenite phase.

The aim of the present work is to compare the phase composition and hyperfine properties of three samples of the  $\text{Fe}_{1-x}\text{Ni}_x$  system, obtained by mechanical alloying and then sintering. According to our knowledge, no work has been reported previously on these alloys prepared by this route.

## 2 Experimental method

Pure carbonyl Fe powder (99.9%) and electrolytic Ni powder (99.9%) were used as the starting materials.  $\text{Fe}_{100-x}\text{Ni}_x$  samples with  $22.5 \leq x \leq 40.0$  were alloyed under vacuum for 10, 24, 48 and 72 h by MA in a planetary ball mill (Fritsch “Pulverisette 5”) using hardened chromium steel vials and balls. The ball mass-to-powder mass (BM/PM) ratio was about 20:1. Part of the final powders were used for be sintered at 1,000°C during 1 h. The MA powders and those obtained after sintering were characterized by X-ray diffraction (XRD) using a Rigaku diffractometer with the  $\text{CuK}\alpha$  radiation and Mössbauer spectrometry (MS) by collecting the spectra at room temperature (RT) with a conventional transmission spectrometer using a  $^{57}\text{Co}$  (Rh) source and an  $\alpha$ -Fe foil as calibration sample. The XRD patterns were refined by the

**Fig. 1** XRD patterns for  $\text{Fe}_{70.0}\text{–Ni}_{30.0}$  samples alloyed during 10, 24, 48 and 72 h



Rietveld Method using the MAUD program [21] and the Mössbauer spectra were fitted by using the MOSFIT program [22].

### 3 Experimental results and discussion

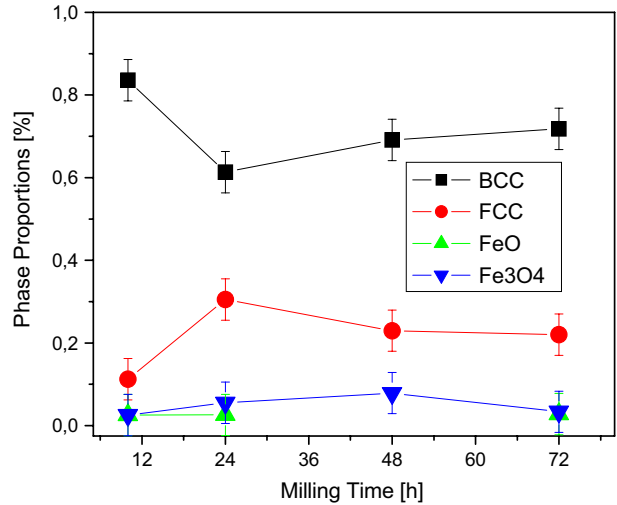
Figure 1 illustrated the XRD patterns of the 30.0 at.% Ni samples milled during different times and then sintered. It can be noted the coexistence of two phases in all the studied samples, BCC and FCC and no appreciable changes with the milling time can be observed. In some sintered samples small quantities of  $\text{FeO}$  and  $\text{Fe}_3\text{O}_4$  oxides appear. Different microstructural models were proposed for the refinement of the patterns and the better description is obtained assuming pseudo-cubic grains for BCC and FCC phases.

Figure 2 shows the behavior of the volumetric percentage of the detected phases as a function of the Ni concentration. The coexistence of the BCC and FCC phases is obtained for all the samples and of the  $\text{FeO}$  and  $\text{Fe}_3\text{O}_4$  oxides in some ones.

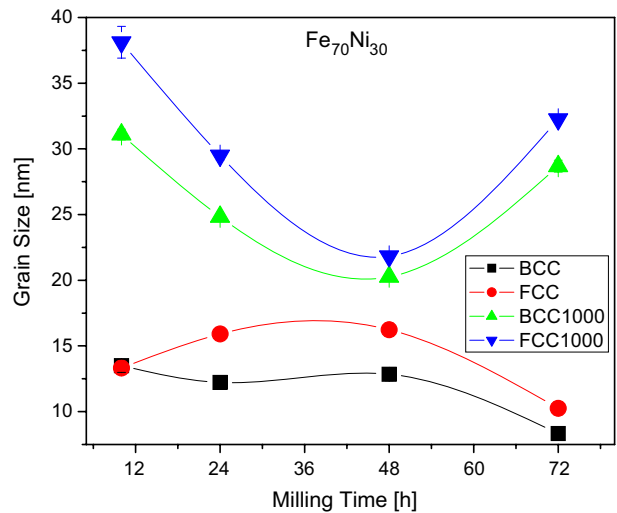
The comparison between the obtained grain sizes for the BCC and FCC phases of the samples obtained by MA and those sintered is shown in Fig. 3. Clearly it can be noted that the grain sizes of the sintered samples (between 20 and 40 nm) are larger than that obtained for the AM samples (between 8 and 20 nm). This enhancement of the grain size is induced by the thermal treatment. Besides, the grain size systematically decreases between 10 and 48 h of mill and then it increases between 48 and 72 h. The reduction of the grains of the phases BCC and FCC can be related with the presence of oxides, which increase the fragility of the particles of the powder.

Figure 4 shows the behavior of the volumetric percentage of the detected phases as a function of the milling time for the samples with 22.5 and 40.0 at.% Ni MA and sintered. It can be noted that the BCC and FCC phases coexist for the sample with  $x = 22.5$ , the content of which decreases and increases as the Ni content increases, respectively. For the sample with  $x = 40.0$  the BCC phase is not

**Fig. 2** Phase proportions obtained from the XRD patterns of the  $\text{Fe}_{70}\text{Ni}_{30}$  MA and then sintered samples



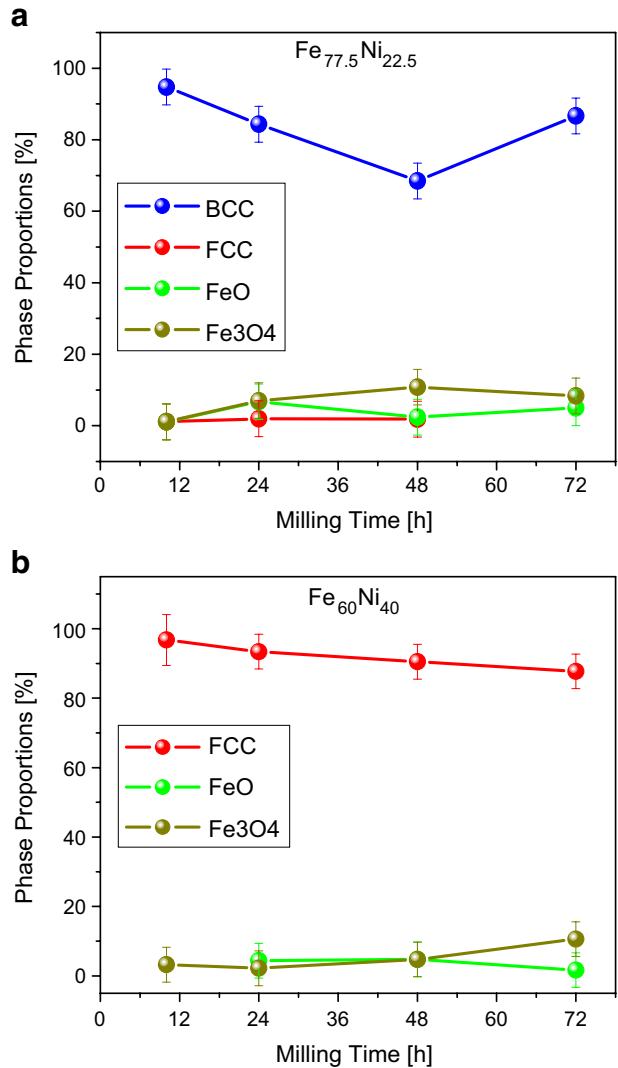
**Fig. 3** Grain size vs. milling time of the Fe–Ni (BCC) and Fe–Ni (FCC) phases obtained from the refinement of the XRD patterns of MA, and MA plus sintering  $\text{Fe}_{70}\text{Ni}_{30}$  samples



detected. Some samples show the  $\text{FeO}$  and  $\text{Fe}_3\text{O}_4$  oxides, which must be due to fails in the Argon flux during the thermal treatment and/or trapped air inside the powders.

The RT Mössbauer spectra which are presented in Fig. 5 were fitted following a recent method proposed for this type of samples [20], which include two hyperfine magnetic field distributions (HMFBDs) and a singlet, in addition to a small preferential orientation of the Fe magnetic moments. Some samples shows the paramagnetic doublet corresponding to  $\text{FeO}$  and two sextets corresponding to the ferrimagnetic

**Fig. 4** Phase proportions vs. milling time obtained from XRD patterns for the  $\text{Fe}_{77.5}\text{Ni}_{22.5}$  and  $\text{Fe}_{60.0}\text{Ni}_{40.0}$  sintered samples



$\text{Fe}_3\text{O}_4$  phase in according with XRD results. The best agreement between the experimental and the calculated spectra was obtained when a maximum field of about 32T was taking for the FCC HMFDF, a small overlap between the HMFDFs was permitted and two different isomer shifts values were used. Finally, the single line is due to the FCC Fe–Ni paramagnetic grains with high Fe content [8, 11, 21]. It can be noted also that for the sample with lower Ni content (22.5 at.%) the bigger contribution to the spectral area corresponds to the HMFDF of the BCC phase. For the case of the sample with bigger Ni content (40 at.%) the mayor spectral area corresponds to the HMFDF of the FCC phase. The MS results obtained for the samples with  $x = 22.5$  and 30 are in according with those obtained by XRD. For the  $x = 40$  sample the BCC ferromagnetic phase was detected by MS and was not

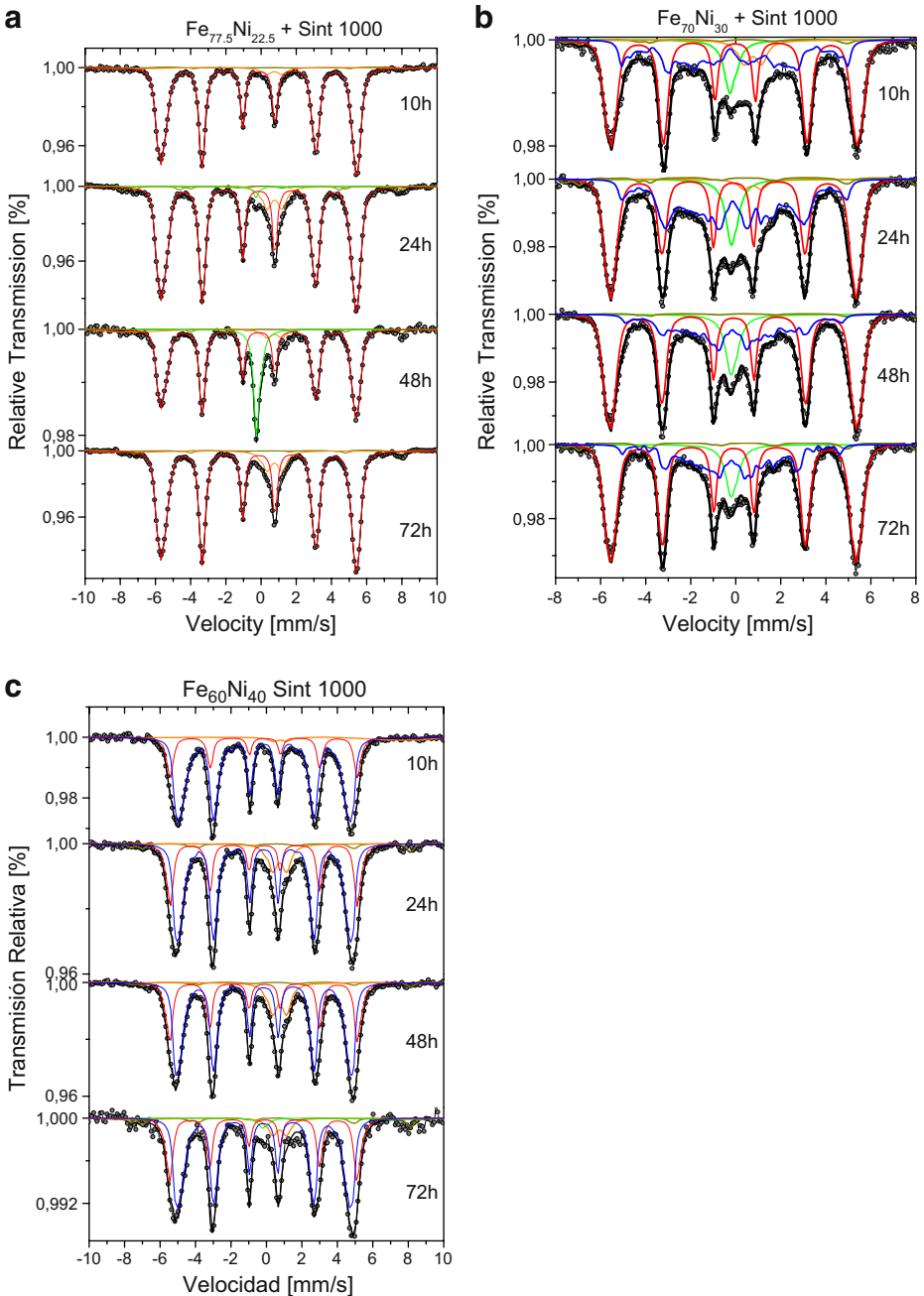


**Fig. 5** RT Mössbauer spectra of  $\text{Fe}_{77.5}\text{Ni}_{22.5}$ ,  $\text{Fe}_{70.0}\text{Ni}_{30.0}$  and  $\text{Fe}_{60.0}\text{Ni}_{40.0}$  sintered samples

detected by XRD. Then this phase appears with a volume fraction lower than 2%, but this phase presents more Fe content than that of the FCC phase explaining in this way its appearing in the MS.

**Fig. 6** HMFDS obtained for the  $\text{Fe}_{100-x}\text{Ni}_x$  samples with 22.5, 30.0 and 40.0 milled during 10 h and sintered. The lines are a guide for the eyes

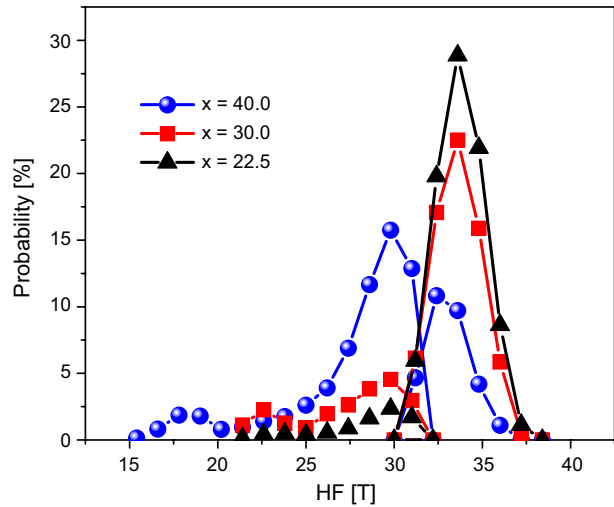


Figure 6 shows the HMFDS estimated from the proposed fit model and after considering the texture effect. It can be noted two principal domains: the high field component is attributed to the BCC Fe–Ni ferromagnetic grains [9], while the other one (lower field values) is ascribed to the FCC Fe–Ni ferromagnetic grains [9].

#### 4 Conclusions

The XRD and MS studies of samples of the  $\text{Fe}_{100-x}\text{Ni}_x$  system with  $x = 22.5, 30.0$  and  $40.0$  prepared by MA, and MA and then sintering show that the structural and magnetic properties of samples prepared by these two routes are very similar. However, two differences can be detected as a consequence of the heat treatment: it stabilize the FCC phase and increase the grain size. These small differences permit to conclude that the MA samples of the Fe–Ni system will preserve their magnetic and structural properties if they will be compacted and sintered in order to manufacture pieces for different applications.

**Acknowledgements** The authors would like to thank ECOS-NORTE and Colciencias, Colombian Agency, and Universidad del Valle, for financial support given to the Excellence Center for Novel Materials (ECNM), under contract no.043–2005. They are very grateful to A.M. Mercier from UMR CNRS 6010 Université du Maine for performing XRD measurements.

#### References

1. Johnson, C.E., et al.: Proc. Phys. Soc. Lond. **81**, 1079 (1963)
2. Gonser, Y., et al.: J. Magn. Magn. Mater. **10**, 244 (1979)
3. Window, B.: J.Phys. F **4**, 329 (1974)
4. Billard, L., et al.: Solid State Commun. **17**, 113 (1975)
5. Hesse, J., Müller, J.B.: Solid State Commun. **22**, 637 (1977)
6. Kuhrt, C., Schultz, L.: J. Appl. Phys. **73**, 1975 (1993)
7. Kuhrt, C., Schultz, L.: J. Appl. Phys. **73**, 6588 (1993)

8. Scorzelli, R.B.: *Hyperfine Interact.* **110**, 143 (1997)
9. Hong, L., Fultz, B.: *J. Appl. Phys.* **79**, 3946 (1993)
10. Baldokhin, Yu.V., Tcherdyntsev, V.V., Kaloshin, S.D., Kochetov, G.A., Pustov, Yu.A.: *J. Magn. Magn. Mater.* **203**, 313 (1999)
11. Lapina, T.M., Shabashov, V.A., Sagaradze, V.V., Arbuzov, V.L.: *Mater. Sci. Forum* **294–296**, 767 (1999)
12. Kaloshin, S.D., Tcherdyntsev, V.V., Tomilin, I.A., Baldokhin, Yu.V., Shelekhov, E.V.: *Physica B* **299**, 236 (2001)
13. Tcherdyntsev, V.V., Kaloshin, S.D., Tomilin, I.A., Shelekhov, E.V., Baldokhin, Yu.V.: *Nanostruct. Mater.* **12**, 139 (1999)
14. Luborsky, F.E.: *J. Appl. Phys.* **32**, 171S (1961)
15. Herzer, G.: *J. Magn. Magn. Mater.* **112**, 258 (1992)
16. Benjamin, J.S.: *Sci. Am.* **234**, 40 (1976)
17. Hellstern, E., Schultz, L.: *J. Appl. Phys.* **63**, 1408 (1988)
18. Suryanarayana, C.: *Prog. Mater. Sci.* **46**, 1–184 (2001)
19. Hellstern, E., Fecht, H.J., Fu, Z., Johnson, W.L.: *J. Appl. Phys.* **65**, 305 (1989)
20. Valderutem, J.F., Pérez Alcázar, G.A., Greneche, J.M.: *J. Phys. Condens. Matter* **20**, 485204 (2008)
21. Lutterotti, L., Matthies, S., Wenk, H.R.: In: *Proceedings of the Twelfth International Conference on Texture of Materials (ICOTOM-12)*, vol. 2, p. 1599 (1999)
22. Varret, F., Teillet, J.: Unpublished Mosfit Program (1976)